AGU PUBLICATIONS

Geophysical Research Letters

RESEARCH LETTER
10.1002/2017GL076694

Key Points:
- The negative linear relationship between earthquake *b*-values and crustal stresses is verified in a young orogenic belt for the first time
- A high correlation between the *b*-value and stress is derived from a complete earthquake catalog regionally
- *b*-values could serve as stress indicators in a young orogenic belt

Correspondence to:
Y.-M. Wu,
drymwu@ntu.edu.tw;
yihmin.wu@gmail.com

Citation:
Wu, Y.-M., Chen, S. K., Huang, T.-C., Huang, H.-H., Chao, W.-A., & Koulakov, I. (2018). Relationship between earthquake *b*-values and crustal stresses in a young orogenic belt. *Geophysical Research Letters*, *45*, 1832–1837. https://doi.org/10.1002/2017GL076694

Received 7 DEC 2017
Accepted 5 FEB 2018
Accepted article online 12 FEB 2018
Published online 24 FEB 2018

Relationship Between Earthquake *b*-Values and Crustal Stresses in a Young Orogenic Belt

Yih-Min Wu[1,2,3], Sean Kuanhsiang Chen[1], Ting-Chung Huang[1], Hsin-Hua Huang[2], Wei-An Chao[4], and Ivan Koulakov[5,6]

[1]Department of Geosciences, National Taiwan University, Taipei, Taiwan, [2]Institute of Earth Sciences, Academia Sinica, Taipei, Taiwan, [3]National Center for Research on Earthquake Engineering, NARLabs, Taipei, Taiwan, [4]Department of Civil Engineering, National Chiao Tung University, Hsinchu, Taiwan, [5]Trofimuk Institute of Petroleum Geology and Geophysics, SB RAS, Novosibirsk, Russia, [6]Department of Geology and Geophysics, Novosibirsk State University, Novosibirsk, Russia

Abstract It has been reported that earthquake *b*-values decrease linearly with the differential stresses in the continental crust and subduction zones. Here we report a regression-derived relation between earthquake *b*-values and crustal stresses using the Anderson fault parameter ($A\phi$) in a young orogenic belt of Taiwan. This regression relation is well established by using a large and complete earthquake catalog for Taiwan. The data set consists of *b*-values and $A\phi$ values derived from relocated earthquakes and focal mechanisms, respectively. Our results show that *b*-values decrease linearly with the $A\phi$ values at crustal depths with a high correlation coefficient of -0.9. Thus, *b*-values could be used as stress indicators for orogenic belts. However, the state of stress is relatively well correlated with the surface geological setting with respect to earthquake *b*-values in Taiwan. Temporal variations in the *b*-value could constitute one of the main reasons for the spatial heterogeneity of *b*-values. We therefore suggest that *b*-values could be highly sensitive to temporal stress variations.

1. Introduction

The earthquake size distribution in the Earth's crust commonly follows the Gutenberg-Richter power law (Gutenberg & Richter, 1944): $\log_{10}N = a - bM$, where a is the total number of earthquakes, b is the relative earthquake size distribution, and N is the number of earthquakes with a magnitude equal to or greater than M. Here the *b*-value governs the slope of the power law, and it is used to describe the frequency of the earthquake size distribution. In other words, a high *b*-value means a predominance of small earthquakes; conversely, a low *b*-value means that large earthquakes dominate over smaller earthquakes. The variations in *b*-values both spatially and temporally are generally regarded as clues for large earthquake precursors (e.g., Smith, 1981). The spatial variations in the *b*-value have been reported to vary with different stress regimes worldwide, particularly in California of the USA, Japan (Schorlemmer et al., 2005), and Italy (Gulia & Wiemer, 2010). These studies indicate that normal and thrust faulting regions have higher and lower *b*-values, respectively, while strike-slip faulting regions have intermediate *b*-values. This phenomenon may imply that the *b*-value acts as a stress meter depending inversely on the differential stress (Schorlemmer et al., 2005). This hypothesis has been supported by laboratory rock fracture experiments showing that the *b*-values of acoustic emission events decrease linearly with an increase in the differential stress ($\sigma_1 - \sigma_3$) (Amitrano, 2003; Goebel et al., 2013; Scholz, 1968). It has also been verified that earthquake *b*-values decrease inversely with the differential stress in the continental crust (Scholz, 2015). For subduction zones, Scholz (2015) also reported a negative linear relation between the *b*-value and differential stress. The relationship between the *b*-value and stress could be very important if it could be well established regionally. Thus, *b*-values could be effective in monitoring spatiotemporal stress variations in the crust. However, the establishment of the abovementioned relationship strongly depends on comparable stress measurements for *b*-value determinations.

The island of Taiwan constitutes a young orogenic belt that initiated at 3–5 Ma (Teng, 1990) when the Philippine Sea Plate began colliding with the Eurasian Plate with a convergence rate of ~82 mm/yr at an azimuth of ~310° (Yu et al., 1997) (Figure 1). This plate convergence has created six major geological provinces on this island. In Figure 1, the Longitudinal Valley (LV) in the southeast represents the suture zone between the Eurasian and Philippine Sea Plates. The eastern side of the LV consists of the Coastal Range (CoR). The

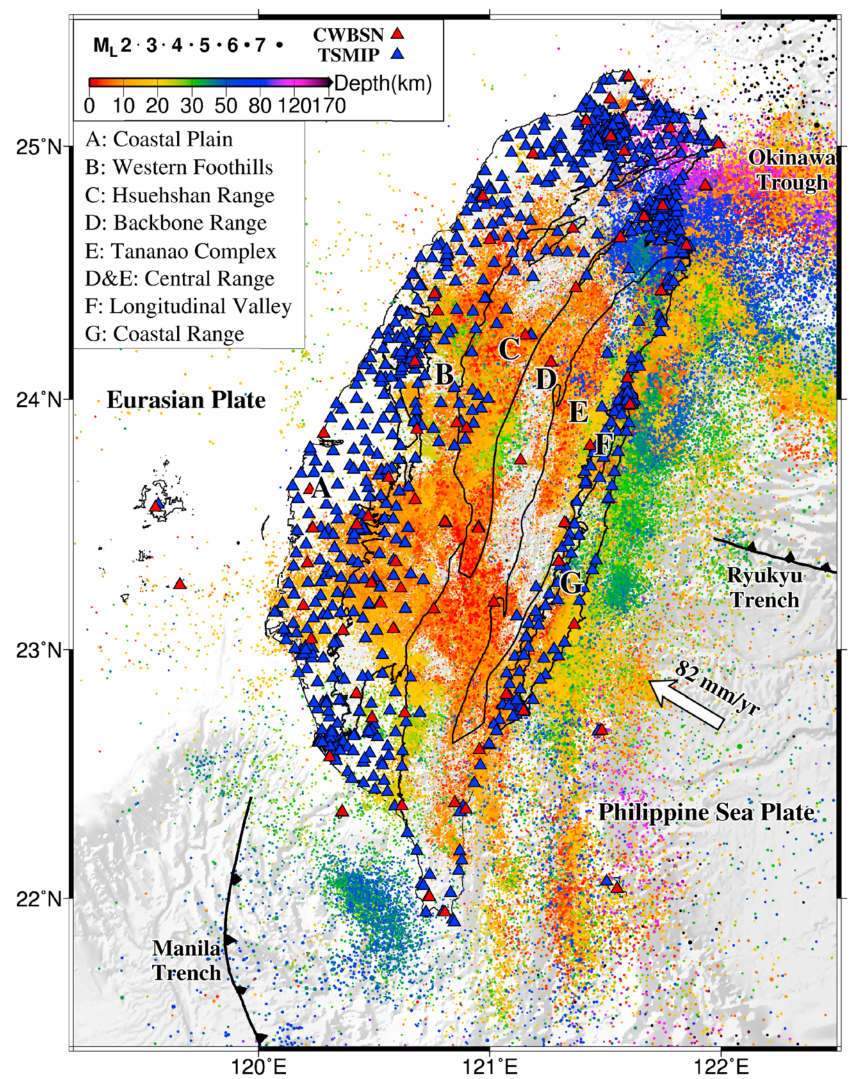

Figure 1. Tectonic settings, seismic networks, and seismicity in the Taiwan region. The white arrow indicates the rate of plate convergence between the Eurasian and Philippine Sea Plates. Major geological provinces on Taiwan Island are marked by black curves and are labeled from A to G. The two seismic networks are colored using different triangles. CWBSN: Central Weather Bureau Seismic Network; TSMIP: Taiwan Strong Motion Instrumentation Program. The colored dots show the relocated hypocenters from 1994 to 2011 based on Wu, Chang, et al. (2008). The sizes are proportional to the magnitude.

western side of the LV can be classified into four geological belts from west to east: the Coastal Plain, the Western Foothills (WF), the Hsueshan Range (HR), and the Central Range (CeR). Additionally, the rapid convergence rate has resulted in strong earthquake activities in this young orogenic belt (Figure 1). These earthquakes are being recorded by a dense seismic network known as the Central Weather Bureau Seismic Network (CWBSN) (Figure 1), which is the agency responsible for earthquake monitoring in Taiwan. A large data set of *P* and *S* wave arrivals, first motion polarities, and *S-P* times from the Taiwan Strong-Motion Instrumentation Program (Figure 1) are combined with the data set from the CWBSN. This overall data set provides a large and relatively complete earthquake relocation catalog (Wu, Chang, et al., 2008) as well as a first-motion focal mechanism catalog (Wu, Zhao, et al., 2008) for further seismological research. For example, focal mechanism catalogs are effective for determining the principal stress tensors of the crust (Hsu et al., 2009; Wu et al., 2010). A stress tensor field together with styles of faulting in the region of Taiwan is recently reported by Chen et al. (2017), showing an improved spatial resolution of the state of stress and the stress

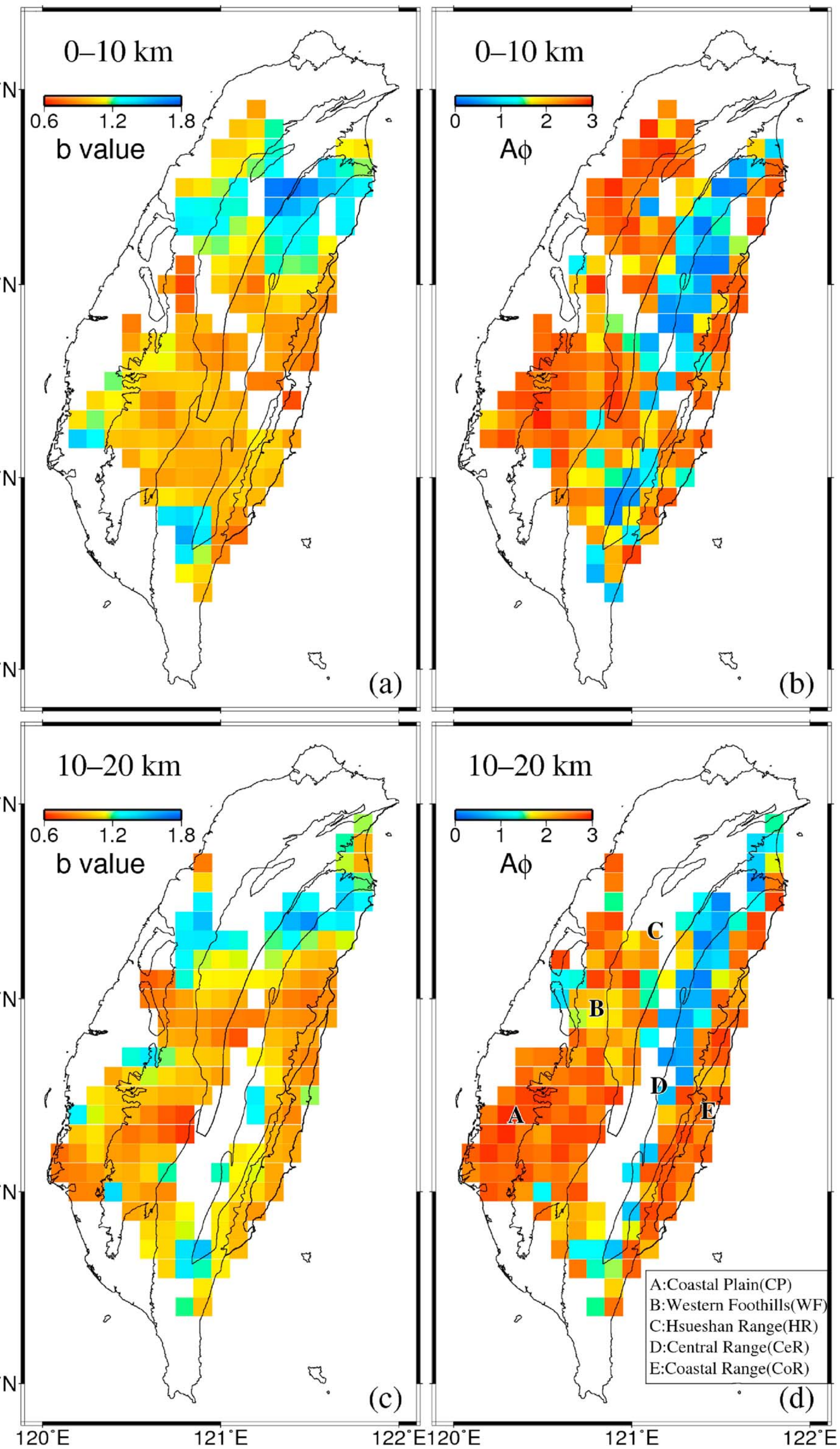

Figure 2. Map view of earthquake *b*-values and Anderson fault parameters ($A\phi$) in the Taiwan region. The hollow grid nodes denote regimes with insufficient data for a stress tensor inversion (Chen et al., 2017).

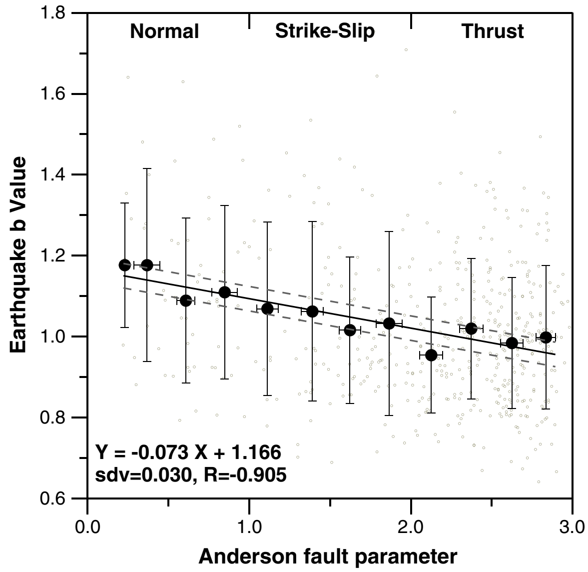

Figure 3. Negative linear relationship between earthquake *b*-values and Anderson fault parameters ($A\phi$) in the Taiwan region. The small white and large black circles represent the raw and grouped data, respectively. The horizontal and vertical bars across each black circle denote one standard deviation of the $A\phi$ and *b*-values, respectively. The solid and dashed lines show the best fitting solutions and their one standard deviation, respectively.

regime in the crust. The data set provides a good opportunity to verify the relationship between the *b*-value and crustal stresses in a young orogenic belt.

2. Stress and *b*-Values in the Taiwan Orogenic Belt

Chen et al. (2017) inverted the crustal stress tensors in Taiwan region from a total of 7,939 focal mechanisms from 1991 to 2015, by employing the spatial and temporal stress inversion algorithm (Hardebeck & Michael, 2006). From the results of spatial and temporal stress inversion, the stress rations (R) derived from directions and magnitudes of three principal stress axes in the grid cell size of 0.1° × 0.1° × 10 km are used to estimate the corresponding Anderson fault parameter ($A\phi$) (Chen et al., 2017). $A\phi$ value is used to describe stress regimes (e.g., Hardebeck & Hauksson, 2001) as defined by Simpson (1997) in the following: $A\phi = (n + 0.5) + (-1)^n \times (R - 0.5)$, where R is the stress ratio $[R = (\sigma_1 - \sigma_2)/(\sigma_1 - \sigma_3)]$ and n is the constant determined from the rake angles such that n = 0, 1, and 2 for normal, strike slip, and thrust type, respectively. The rake angles (λ) from double-coupled focal mechanisms are classified into the three types according to a given range of ±40° from pure events, that is, $\lambda = -90°$ as normal, $\lambda = 0°$, and ±180° as strike slip and $\lambda = 90°$ as thrust events. Each rake angle in the given grid cell is determined by a moment tensor summation technique (Kostrov, 1974) from focal mechanisms within the grid cell or within an area twice the grid cell for grid nodes where focal mechanism is less than 10 events. Since the $A\phi$ value includes parameters of the differential stress and rake angles, it is a suitable index for constraining the relationship between stresses and earthquake *b*-values in Taiwan. We note that the one standard deviation for stress ratios and rake angles from Chen et al. (2017) are approximately 0.22 and 20°, respectively. The $A\phi$ value ranges from 0 to 1, from 1 to 2, and from 2 to 3 for normal, strike slip, and thrust faulting regimes, respectively.

In this study, we used a relocated earthquake catalog (Wu, Chang, et al., 2008) from 1994 to 2011 to estimate the *b*-values in the region of Taiwan. This data period was selected because the CWBSN was operated in a triggered-recording mode before 1994, and the operation system was upgraded after 2011. The relocated catalog includes 369,952 events in the Taiwan region from 1994 to 2011 (Figure 1). The magnitudes range from M_L 0.6 to 7.3. The depth range is between 0.5 and 275 km, and most of the events are shallower than 40 km. To accurately estimate the *b*-values from background seismicity, temporal and spatial double-link cluster analyses (e.g., Wu & Chiao, 2006; Wu, Chen, et al., 2008) were used to remove the aftershocks from the data set. We removed the aftershock sequences for main shocks with $M_L > 4.0$ with linking parameters of 3 days and 5 km. To evaluate the reliability of the catalog, we calculated the spatial distribution of the magnitude completeness (M_C) by using the maximum curvature approach (Wiemer & Wyss, 2000). We used a maximum-likelihood method (Aki, 1965) to determine the *b*-values with the same grid cell size as $A\phi$ (Chen et al., 2017), that is, horizontal and vertical grid cells of 0.1° and 10 km, respectively, at depths between 0 and 40 km. We required at least 50 events with magnitudes larger than M_C for a *b*-value determination.

The *b*-values and $A\phi$ values in the Taiwan region are shown individually in Figure 2 above a depth of 20 km, which is the depth extent in the crust with the most solutions of $A\phi$ values (Chen et al., 2017). We found that the lowest *b*-values are located in the southern WF and in the CoR, and they correlate with the highest $A\phi$ values as in a thrust faulting regime. In contrast, the highest *b*-values are founded in the northern CeR corresponding to the lowest $A\phi$ values as in a normal faulting regime. Additionally, the *b*-values are intermediate in the southern HR and CeR, and they partially correlate with intermediate $A\phi$ values as in a strike-slip faulting regime. These observations are consistent with the phenomenon that *b*-values decrease linearly with the stress regime from normal to strike slip to thrust faulting regimes (Gulia & Wiemer, 2010; Schorlemmer et al., 2005).

To find a relationship between the $A\phi$ and b-values for the Taiwan orogenic belt, we used a least squares linear regression approach to search for a best fitting line for the two data sets. Due to the scattering in the raw data (Figure 3), we grouped the data in an $A\phi$ value interval of 0.25 and calculated the mean values to search for the best fitting line associated with those values. In Figure 3, we can observe a clear negative linear relationship between the $A\phi$ and b-values based on the mean values as follows: $b = -0.073A\phi + 1.166$. The correlation coefficient is -0.905. The grouped data in this negative linear fitting display relatively stable results, with a minimum one standard deviation of 0.03.

3. Discussion and Conclusions

Earthquake b-values have been found to decrease linearly with crustal stresses in the continental crust globally (Scholz, 1968, 2015). However, in this study, this linear relationship is reported for the first time for a young orogenic belt using a large and relatively complete data set from Taiwan. A better correlation coefficient of -0.91 was achieved in this study compared with that of -0.77 determined from a study of the global continental crust (Scholz, 2015). This difference in the correlation coefficient may result from the difference in the tectonic setting. The data set generated by Scholz (2015) for the continental crust included several different tectonic regions. If they were estimated individually, each data set could have own linear relationship with each better correlation coefficient. It implies the existence of different negative linear relationships between the b-values and crustal stresses in different tectonic settings. In Figure 1 of Scholz (2015), the data in the Japan region followed a lower slope of negative linear relationship that consistently differed from those in other regions upon closer inspection. The lower slope with high correlation coefficient is consistent with our result which b-values decrease inversely with $A\phi$ values in a lower slope (Figure 3). Japan is a tectonic region mainly characterized by thrust to strike-slip faulting (Wesnousky et al., 1982), which is similar to the $A\phi$ values as presented in Taiwan region (Figure 3). This verified that the negative linear relationship estimated from our study is reliable, and it is much more robust based on the completeness of regional data set.

Although a better correlation coefficient is obtained in this study, our large data set shows a scattering of 0.7 in the b-values with the $A\phi$ values (Figure 3), which is higher than the simple data sets combined by Scholz (2015) at about a scattering of 0.3 in the b-values. The variations in b-values both in space and time, which has been reported from analysis of the earlier data set in Taiwan (Chan et al., 2012; Wu & Chiao, 2006; Wu, Chen, et al., 2008), could be one of the reasons causing that scattering. The temporal variations of b-values were estimated to be a scattering of 0.3 in long-term average from Figure 4 of Wu and Chiao (2006) and Figure 3 of Wu, Chen, et al. (2008). Note that the temporal variations show episodic, larger scattering of 0.5 in b-values in that two figures. Chan et al. (2012) investigated the spatial and temporal variations in b-values before 23 $M_L \geq 6.0$ earthquakes in the Taiwan region, suggesting that the spatial variation of b-values is prior to the earthquakes, which means lower b-values occurring predominately in/around the epicenters of impending earthquakes. The previous observations, highlighting a spatiotemporal variation of earthquake b-values in the crust, may explain a scattering of 0.7 in the b-values with the $A\phi$ values from a longer observation in this study.

In addition, our results show that the earthquake b-values in Taiwan do not correlate well with the surface geological setting with respect to the $A\phi$ values. Based on the inferred stress regimes of Taiwan (Chen et al., 2017) above the depths of 20 km (Figure 2), the Coastal Plain, WF, and HR are dominated by thrust faulting, and the CoR and CeR are dominated by normal and a mixture of thrust and strike-slip faulting, respectively. However, earthquake b-values in Taiwan show spatial heterogeneity regionally and do not coherently follow the spatial distribution of surface geological settings (Figure 2). The spatial heterogeneity in b-values could directly reveal variations of differential stress in the crust, since we have found that locations of the highest and lowest b-values corresponding to the lowest and highest $A\phi$ values, respectively, are highly overlapped. These observations, coupled with the previous result of spatiotemporal variation in b-values (Chan et al., 2012), may imply that earthquake b-values are more sensitive to detect the variations in confining/pore pressure in the crust than differential stresses ($A\phi$ values) do. We therefore suggest that b-values could be highly sensitive to temporal stress variations. Nevertheless, the features can only reflect that crustal stress is relatively stable in the space and time with respect to earthquake b-values in Taiwan region. Note that the occurrence of a large earthquake, such as the 1999 M_w 7.6 Chi-Chi earthquake, could also cause significant changes in the stress regime at Taiwan (Wu et al., 2010).

The relationship between earthquake *b*-values and crustal stress is established for the first time in a young orogenic belt in this study. We find that spatial *b*-values decrease inversely with the $A\phi$ values in the crust. High and low *b*-value regions correlate with normal and thrust faulting regimes, respectively, and intermediate *b*-values partially correlate with strike-slip faulting regimes. The negative linear relationship between crustal stresses and *b*-values has a high correlation coefficient of −0.9. This relationship will be helpful for monitoring variation in the state of stress in the Taiwan region and other young orogenic belts when stress measurements in the crust are lacking.

Acknowledgments
We wish to thank the Central Weather Bureau (CWB) for providing the seismic data. We also wish to thank the constructive comments from reviewers and editor. This research was supported by the Ministry of Science and Technology (MOST) of Taiwan. Ivan Koulakov is supported by the RFBR 18-55-52003_MNT_a.The author gratefully acknowledges Wessel et al. (2013) for the Generic Mapping Tools (GMT) software that was used to plot some of the figures. Relocation earthquake catalog, focal mechanism catalog, and Anderson fault parameter ($A\phi$) of the Taiwan region are used in this study can be obtained from http://seismology.gl.ntu.edu.tw/download.htm.

References

Aki, K. (1965). Maximum likelihood estimate of b in the formula logN = a − bM and its confidence. *Bulletin of the Seismological Society of America*, *43*, 237–239.

Amitrano, D. (2003). Brittle-ductile transition and associated seismicity: Experimental and numerical studies and relationship with the b value. *Journal of Geophysical Research*, *108*(B1), 2044. https://doi.org/10.1029/2001JB000680

Chan, C. H., Wu, Y. M., Tseng, T. L., Lin, T. L., & Chen, C. C. (2012). Spatial and temporal evolution of b-values before large earthquakes in Taiwan. *Tectonophysics*, *532-535*, 215–222. https://doi.org/10.1016/j.tecto.2012.02.004

Chen, S. K., Wu, Y. M., Hsu, Y. J., & Chan, Y. C. (2017). Current crustal deformation reassessed by cGPS strain-rate estimation and focal mechanism stress inversion. *Geophysical Journal International*, *210*(1), 228–239. https://doi.org/10.1093/gji/ggx165

Goebel, T. H. W., Schorlemmer, D., Becker, T. W., Dresen, G., & Sammis, C. G. (2013). Acoustic emissions document stress changes over many seismic cycles in stick-slip experiments. *Geophysical Research Letters*, *40*, 2049–2054. https://doi.org/10.1002/grl.50507

Gulia, L., & Wiemer, S. (2010). The influence of tectonic regimes on the earthquake size distribution: A case study for Italy. *Geophysical Research Letters*, *37*, L10305. https://doi.org/10.1029/2010GL043066

Gutenberg, B., & Richter, C. (1944). Frequency of earthquake in California. *Bulletin of the Seismological Society of America*, *34*(4), 185–188.

Hardebeck, J. L., & Hauksson, E. (2001). The crustal stress field in southern California and its implications for fault mechanics. *Journal of Geophysical Research*, *106*, 21,859–21,882. https://doi.org/10.1029/2001JB000292

Hardebeck, J. L., & Michael, A. J. (2006). Damped regional-scale stress inversions: Methodology and examples for southern California and the Coalinga aftershock sequence. *Journal of Geophysical Research*, *111*, B11310. https://doi.org/10.1029/2005JB004144

Hsu, Y. J., Yu, S. B., Simons, M., Kuo, L. C., & Chen, H. Y. (2009). Interseismic crustal deformation in the Taiwan plate boundary zone revealed by GPS observations, seismicity, and earthquake focal mechanisms. *Tectonophysics*, *479*(1-2), 4–18. https://doi.org/10.1016/j.tecto.2008.11.016

Kostrov, V. (1974). Seismic moment and energy of earthquakes and seismic flow of rocks. *Physics of the Solid Earth*, *1*, 13–21.

Scholz, C. H. (1968). The frequency-magnitude relation of microfracturing in rock and its relation to earthquakes. *Bulletin of the Seismological Society of America*, *58*(1), 399–415.

Scholz, C. H. (2015). On the stress dependence of the earthquake b value. *Geophysical Research Letters*, *42*, 1399–1402. https://doi.org/10.1002/2014GL062863

Schorlemmer, D., Wiemer, S., & Wyss, M. (2005). Variations in earthquake-size distribution across different stress regimes. *Nature*, *437*(7058), 539–542. https://doi.org/10.1038/nature04094

Simpson, R. (1997). Quantifying Anderson's fault types. *Journal of Geophysical Research*, *102*, 17,909–17,919. https://doi.org/10.1029/97JB01274

Smith, W. D. (1981). The b-value as an earthquake precursor. *Nature*, *289*(5794), 136–139. https://doi.org/10.1038/289136a0

Teng, L. S. (1990). Geotectonic evolution of late Cenozoic arc continent collision in Taiwan. *Tectonophysics*, *183*(1-4), 57–76. https://doi.org/10.1016/0040-1951(90)90188-E

Wesnousky, S. G., Scholz, C. H., & Shimazaki, K. (1982). Deformation of an island arc: Rates of moment release and crustal shortening in intraplate Japan determined from seismicity and quaternary fault data. *Journal of Geophysical Research*, *87*, 6829–6852. https://doi.org/10.1029/JB087iB08p06829

Wessel, P., Smith, W. H. F., Scharroo, R., Luis, J. F., & Wobbe, F. (2013). Generic mapping tools: Improved version released. *Eos, Transactions American Geophysical Union*, *94*(45), 409–410. https://doi.org/10.1002/2013EO450001

Wiemer, S., & Wyss, M. (2000). Minimum magnitude of completeness in earthquake catalogs: Examples from Alaska, the Western United States, and Japan. *Bulletin of the Seismological Society of America*, *90*(4), 859–869. https://doi.org/10.1785/0119990114

Wu, Y. M., Chang, C. H., Zhao, L., Teng, T. L., & Nakamura, M. (2008). A comprehensive relocation of earthquakes in Taiwan from 1991 to 2005. *Bulletin of the Seismological Society of America*, *98*(3), 1471–1481. https://doi.org/10.1785/0120070166

Wu, Y. M., Chen, C. C., Zhao, L., & Chang, C. H. (2008). Seismicity characteristics before the 2003 Chengkung, Taiwan Mw 6.8 earthquake. *Tectonophysics*, *457*(3-4), 177–182. https://doi.org/10.1016/j.tecto.2008.06.007

Wu, Y. M., & Chiao, L. Y. (2006). Seismic quiescence before the 1999 Chi-Chi, Taiwan Mw 7.6 earthquake. *Bulletin of the Seismological Society of America*, *96*(1), 321–327. https://doi.org/10.1785/0120050069

Wu, Y. M., Hsu, Y. J., Chang, C. H., Teng, L. S., & Nakamura, M. (2010). Temporal and spatial variation of stress field in Taiwan from 1991 to 2007: Insights from comprehensive first motion focal mechanism catalog. *Earth and Planetary Science Letters*, *298*(3-4), 306–316. https://doi.org/10.1016/j.epsl.2010.07.047

Wu, Y. M., Zhao, L., Chang, C. H., & Hsu, Y. J. (2008). Focal mechanism determination in Taiwan by genetic algorithm. *Bulletin of the Seismological Society of America*, *98*(2), 651–661. https://doi.org/10.1785/0120070115

Yu, S. B., Chen, H. Y., & Kuo, L. C. (1997). Velocity field of GPS stations in the Taiwan area. *Tectonophysics*, *274*(1-3), 41–59. https://doi.org/10.1016/S0040-1951(96)00297-1